

1 **Paleoceanographic implications of submarine scours and contourites around ancient**
2 **volcanoes, eastern Great Australian Bight**

3
4 Christopher A-L. Jackson*

5 Craig Magee

6 Esther R. Hunt-Stewart

7
8 *Basins Research Group (BRG), Department of Earth Science & Engineering, Imperial*
9 *College, Prince Consort Road, LONDON, SW7 2BP, UK*

10
11 **corresponding author email: c.jackson@imperial.ac.uk*

12
13 **ABSTRACT**

14
15 Thermohaline oceanic currents control local and global variations in climate, vegetation, and
16 biodiversity. Paleoceanographic studies typically use biostratigraphic and geochemical proxies
17 to reconstruct the dynamics of these currents in Earth's ancient oceans. Here we use 2D seismic
18 reflection data to interrogate the Middle Eocene-to-Recent stratigraphic record of ocean current
19 evolution within the Ceduna Sub-basin, which is located in the eastern Great Australian Bight.
20 These data show that 10–90 m deep, up to 3 km wide erosional scours, and <50 m thick,
21 sediment wave-like bedforms, probably generated by contour currents, are developed
22 throughout this carbonate-dominated succession. The scours are particularly well-developed at
23 one specific stratigraphic level, and define 'moats' encircling Middle Eocene shield volcanoes,
24 which, at that time, formed bathymetric highs. We suggest that sediment erosion, transport,
25 and deposition may record Middle Eocene initiation of the Leeuwin Current, one of the most
26 important ocean currents in the southern hemisphere. Deepest seabed scouring may reflect
27 middle Miocene waxing of the so-called 'proto-Leeuwin Current', possibly driven by changes
28 in ocean circulation patterns caused by the Miocene Global Optimum. The results of this
29 seismic reflection-based study are consistent with results derived from other
30 paleoceanographic proxies, thereby highlighting the key role seismic reflection data have in
31 understanding the occurrence, geographical distribution, and significance of ancient ocean
32 currents.

33
34 *end of abstract*

35

36 By influencing seawater temperature and salinity, ocean current activity controls regional and
37 global trends in climate and biodiversity. Determining past changes in thermohaline circulation
38 patterns in the world's oceans is thus important to understanding how climate and biodiversity
39 varied in deep time and, therefore, may change in the future (cf. "geological analogues" of
40 IPCC, 2007; see also e.g., Henderson, 2002; Wunsch, 2002; Rahmstorf, 2003; Wyrwoll et al.,
41 2009). Paleoceanographic analysis commonly relies on biostratigraphic and geochemical
42 proxy data, which: (i) are expensive to collect, and typically only collected on academic
43 scientific cruises (e.g. IODP); (ii) are spatially limited (i.e. collected over a relatively small
44 area within a discrete stratigraphic intervals); and (iii) do not typically provide a physical (i.e.
45 stratigraphic) record of the initiation, extent, and decay of oceanographic currents (e.g. von
46 Blackenburg, 1999; Henderson, 2002).

47 Seismic reflection data, which can provide relatively high-resolution images of the
48 Earth's subsurface (e.g. Cartwright and Huuse, 2003), provide an additional but hitherto
49 underutilised tool for determining the basin-scale dynamics of ancient ocean currents (e.g.,
50 Boldreel et al., 1998; Davies et al., 2001; Due et al., 2006; Hohbein et al., 2012). For example,
51 seismic data can image large (up to 10's of metre thick, and several hundred-to-tens of
52 kilometres long), contour current-driven bedforms, which document protracted transport and
53 deposition of biogenic or detrital sediment (e.g. Rebesco and Stow, 2001; Stow et al., 2003),
54 and/or scours of comparable depth, width, and length that record periods of net-seabed erosion
55 and sediment redeposition. If integrated with other, more commonly used paleoceanographic
56 proxies, seismic reflection data could form a key part of the oceanographer's toolkit.

57 In this study we use 2D seismic reflection data from the Ceduna Sub-basin, in the
58 eastern Great Australian Bight to map seismic-scale, Middle Eocene-to-Recent scours and
59 bedforms preserved adjacent to Middle Eocene volcanoes. We suggest these scours and
60 bedforms reflect Middle Eocene initiation of the current now known as the Leeuwin Current.
61 Although its age of initiation is debated, the present Leeuwin Current is the longest (5000 km)
62 and one of the most important ocean currents in the southern hemisphere (see below). By
63 providing physical evidence for ocean current activity, the results of our seismic reflection-
64 based analysis at least broadly support studies proposing a Middle Eocene initiation age for the
65 Leeuwin Current. More generically, our study opens up the exciting possibility that industry
66 seismic reflection data, which are freely available for academic use along this and many other
67 continental margins, if integrated with biostratigraphic and geochemical proxies, can help
68 improve our understanding of deep-time dynamics of the Earth's ancient oceans.

69

70 **Geological Setting.** The Ceduna Sub-basin is located in the Bight Basin, offshore southern
71 Australia (Fig. 1A), and formed in response to Jurassic-to-Early Cretaceous rifting and Early
72 Cretaceous-to-Recent, post-rift thermal subsidence. Numerous submarine volcanoes were
73 emplaced during earliest Middle Eocene magmatism at *ca.* 42 Ma (the ‘Bight Basin Igneous
74 Complex’; Schofield & Totterdell, 2008; Jackson, 2012; Magee et al., 2013), with the
75 volcanoes overlapped by the fully marine, Middle Eocene-to-Recent, carbonate-dominated
76 Nullarbor Limestone (Fig. 1B) (Schofield & Totterdell, 2008). Schofield & Totterdell (2008)
77 and Jackson (2012) identify numerous ‘scours’ in the Nullarbor Limestone, although they do
78 not explore their age or origin, their genetic relationship to the Middle Eocene volcanoes, or
79 the potential paleoceanographic significance of their causal current. There are no direct
80 constraints on Middle Eocene-to-Recent water depths in the distal Ceduna Sub-basin, although
81 Jackson (2012) suggests the basin deepened to a few hundred metres during Middle Eocene
82 flooding (see also McGowran et al., 1997; Shafik, 1983; 1990). The interpreted relatively deep-
83 marine setting is consistent with water depth indicators provided by the heights of Eocene
84 clinoforms preserved along the northern basin margin (Feary and James, 1995, 1998;
85 McGowran et al., 1997). The Ceduna Sub-basin lies outboard of the modern day shelf edge in
86 water depths of 200–4000 m; the seabed in the study area is below the influence of the modern
87 Leeuwin Current, which extends to depths of 300 m (Feng et al., 2009).

88

89 **Paleoceanography of the Great Australian Bight.** The Leeuwin Current is the longest (5000
90 km) coastal current in the world and one of the most important ocean currents in the southern
91 hemisphere (Fig. 1A). It is connected to and thus samples the global thermohaline system via
92 the Indonesian Gateway (Feng et al., 2009), flowing southwards along the western coast of
93 Australia and thereafter eastwards into the Great Australian Bight (Fig. 1A) (Cresswell and
94 Golding, 1980). Transporting warm, low-salinity waters derived from the South Equatorial
95 Current, the Leeuwin Current contributes to climatic variations and vegetation patterns (e.g.,
96 Caputi, 2001; Feng et al., 2009; Wyrwoll et al., 2009), and continent-scale biodiversity patterns
97 by transporting otherwise low-latitude fauna to anomalously high latitudes (e.g., Cann and
98 Clarke, 1993; McGowran et al., 1997; Passlow et al., 1997).

99 The Quaternary extent and dynamics of the Leeuwin Current in the Great Australian
100 Bight are relatively well understood (Cresswell and Golding, 1980; Feng et al., 2009; Wyrwoll
101 et al., 2009), whereas its timing of initiation, and its pre-Quaternary eastward ‘reach’ into the
102 Great Australian Bight, remain uncertain. Based on their discovery of warm-water, Eocene

103 microfauna in the Otway Basin, McGowran et al. (1997) suggested an even older, Middle
104 Eocene age of initiation for the Leeuwin Current in the Great Australian Bight, arguing these
105 fauna were likely derived from warm low-latitudes (i.e. via the proto-Leeuwin Current) and
106 not cold high-latitudes (i.e. via the Flinders Current) (Fig. 1A); this interpretation is supported
107 by fully coupled climate model simulations (Huber et al., 2004). However, pre-Early Oligocene
108 initiation of the Leeuwin Current is disputed given that opening of the Tasmanian Gateway,
109 which facilitated eastwards flow of warm ocean waters along southern Australia into the
110 Pacific, did not occur until the Early Oligocene (e.g. Stickley et al., 2004; Wyrwoll et al., 2009).
111 These studies together suggest the proto-Leeuwin Current in some way shaped the Eocene-to-
112 Recent stratigraphic evolution of the Great Australian Bight shelfal regions, although the
113 stratigraphic expression of time-equivalent, basin-centre units, which should also record the
114 initiation and influence of this important ocean current, has yet to be documented.

115 Although Middle Eocene initiation of the Leeuwin Current is disputed, there is
116 evidence from IODP Leg 182 that anomalously warm waters entered the Great Australian
117 Bight during the middle Miocene, possibly in response changes in ocean circulation driven by
118 the Miocene Climatic Optimum (e.g. Savin et al., 1975; Feary and James, 1995, 1998; Gourley
119 and Gallagher, 2004). For example, McGowran et al. (1997) document the ‘Little Barrier Reef’,
120 a thick (350 m), laterally extensive (>475 km long), rimmed carbonate platform developed
121 along the northern margin of the Bight Basin (Fig. 1A).

122
123 **Data and methods.** Our dataset consists of 109 time-migrated, zero-phase, 2D seismic
124 reflection lines that have a cumulative line length of *c.* 13,000 km and cover *c.* 44,000 km² of
125 the central Ceduna Sub-basin (Fig. 1A). The NW- and NE-trending lines are spaced 4–16 km
126 and 4–8 km, respectively (Fig. 2). The Gnarlyknots-1a borehole constrains the age of four key
127 seismic reflections (Horizons A–D; Figs 1B and 3). This borehole also contains well-log data,
128 indicating the Nullarbor Limestone has a p-wave velocity of 2100 m s⁻¹, thereby allowing us
129 to convert measurements in milliseconds two-way time (ms TWT) to metres (cf. Espurt et al.,
130 2009). Extrusive igneous bodies were identified and mapped using the geometric and
131 geophysical criteria outlined by Totterdell & Schofield (2008), Jackson (2012) and Magee et
132 al. (2013). Intra-Nullarbor scours are characterised by erosional surfaces that truncate and are
133 onlapped by, underlying and overlying reflections respectively (Fig. 3). Although seismic data
134 are only 2D and relatively widely spaced, scours and spatially related ‘hummocky’ seismic
135 facies are typically imaged on and can be mapped between, several adjacent seismic lines. In

136 particular, it is clear that the scours are only developed adjacent to and define ‘moats’ that
137 encircle the volcanic vents (see below and Fig. 2).

138

139 **Description of intra-Nullarbor seismic facies.** We define two main stratal units within the
140 Nullarbor Formation (SU1-2), separated by a major erosional surface (Horizon D; Figs 1 and
141 3). The base of SU1 is defined by a high-amplitude, laterally-continuous, positive seismic
142 reflection defining the contact between the Pidinga Formation and the Nullarbor Limestone
143 (i.e. Horizon B), or a series of volcanoes (i.e. Horizon C) (Figs 1B and 3). SU1 comprises the
144 lower part of the Nullarbor Limestone and, away from the volcanoes, is typically characterised
145 by low-to-moderate amplitude, parallel-to-sub-parallel, very continuous reflections (Fig. 3).
146 Closer to the volcanoes (i.e. <2 km), a series of gently-dipping (<4°) reflections are developed
147 in SU1, and these locally display bilateral downlap onto the underlying reflections and thus
148 define convex-up, ‘mounded’ bodies (Figs 3B-D). These inclined reflections, which either dip
149 towards (Fig. 3A) or away (Figs 3C–D) from the volcanoes, typically overlie low-angle (<6°)
150 erosional surfaces, which are up to 2 km wide and display up to 100 m of relief; these surfaces
151 pass laterally into (seismically) conformable surfaces (Fig. 3).

152 The base of SU2 is locally defined by a major erosion surface along which numerous
153 scours are developed (Horizon D; Figs 1–3). These scours locally define a series of ‘moat-like’
154 features that fully or partly encircle 15 of the 57 vents present in the Ceduna Sub-basin (e.g.
155 Fig. 2). The scours have a relief of 10–90 m, extend <3 km from the volcanoes, and their flanks
156 dip 0.1–6.1°, being best-developed around volcanoes that are typically >200 m tall. Some of
157 the scours are asymmetric, consisting of a long, gently dipping outer margin inclined towards
158 the vents and a shorter, more steeply-dipping surface that dips away from the vents (Figs 3B–
159 D). Our 2D seismic data do not allow us to confidently determine if the scours are preferentially
160 developed on one side of the vents (Fig. 2). Two main types of seismic facies fill the scours:
161 (i) high-amplitude, ‘hummocky’ reflections, which have a relief of up to 50 m and a distance
162 of 100–200 m between adjacent hummock crests (Fig. 3B); and (ii) low-to-high amplitude,
163 gently-dipping (<2°), moderately discontinuous to laterally-continuous reflections (Fig. 3). The
164 upper part of SU2 is dominated by low-to-high amplitude, flat-lying to gently-dipping (<2°),
165 laterally-continuous reflections (Fig. 3), with erosionally based packages of chaotic reflections
166 locally being developed.

167

168 **Interpretation of intra-Nullarbor features.** Based on their development in a fully marine
169 succession and given that post-Middle Eocene water depths were probably at least several

170 hundred metres (see Jackson, 2012), it is unlikely the intra-Nullarbor scours and hummocks
171 formed subaerially. Furthermore, the coeval basin margin, which was likely located several
172 hundred kilometres to the north, was carbonate-dominated and constructional (Fig. 1; see also
173 Feary and James, 1995, 1998), suggesting little or no sediment bypass was occurring, and that
174 voluminous, strongly erosional, deep-water gravity currents, such as turbidity currents, did not
175 form the intra-Nullarbor scours and hummocks.

176 Based on their development in a fully marine succession deposited in several hundreds
177 of metres of water, our preferred interpretation is that the scours formed in response to ocean
178 current-related incision of the seabed. Such scours are common in modern seas and oceans,
179 typically in association with channel-related contourite drifts (*sensu* Stow et al., 2002). The
180 spatial restriction of Ceduna Sub-basin scours to within c. 3 km of the volcanoes, strongly
181 suggests the volcanic edifices formed syn-incision bathymetric highs that perturbed the
182 velocity structure of the causal ocean currents. We suggest this perturbation increased current
183 turbulence and, most critically, seabed shear stress, driving localised erosion of the seabed
184 immediately adjacent to the volcanoes (e.g. O'Reilly et al., 2003; MacLachlan et al., 2008).
185 Submarine scours of broadly similar geometry, dimension, and origin are observed adjacent to
186 igneous rock-cored bathymetric highs in the Pisces Reef system, Irish Sea, UK (Callaway et
187 al., 2009), and in the Capel and Faust basins, offshore eastern Australia (Rollet et al., 2012).

188 We interpret that inclined and hummocky reflections developed throughout the
189 Nullarbor Limestone represent dip-oblique and dip-parallel sections, respectively, through
190 sediment wave- or contourite drift-like deposits (cf. Rebesco and Stow, 2001; Stow et al., 2003;
191 Hohbein et al., 2012). Sedimentary bodies like this are commonly associated with seabed
192 scours, being deposited when bottom current energy is low enough to permit sediment
193 reworking within bedforms (e.g. Stow et al., 2002). Like the scours, intra-Nullarbor bedforms
194 are spatially restricted to within a few kilometres of the vents, suggesting they too formed due
195 to volcano-driven perturbations in ocean current velocity and seabed shear stress. In their case,
196 however, an increase in seabed shear stress was only sufficient to rework sediment and not
197 deeply erode the seabed.

198

199 **Implications for the paleoceanographic development of the Great Australian Bight.**

200 Although the Gnarlyknots-1a borehole penetrates the Nullarbor Formation, no biostratigraphic
201 data were collected; as a result, we cannot constrain the age of intra-Nullarbor scours,
202 associated strata, or indeed, the causal current more tightly than 'Middle Eocene-to-Recent'.
203 Furthermore, no paleobathymetric data (e.g. benthic foraminifera) were collected in

204 Gnarlyknots-1a, meaning we have no direct constraints on water depth variations during the
205 Middle Eocene-to-Recent, and thus the depth of formation of the ocean current-related scours
206 and bedforms remains uncertain (see also discussion in Jackson, 2012). Our relatively widely
207 spaced 2D seismic reflection data also do not allow us to confidently determine if intra-
208 Nullarbor scours are preferentially developed on one, most likely the down-current (i.e. lee)
209 side of the seabed obstruction (i.e. the volcanoes), or if the associated bedforms are best-
210 developed on one, most likely the up-current side of the vents, and display down-current
211 accretion (e.g. Callaway et al., 2009; Rollet et al., 2012). Because of this, we do not know the
212 dominant direction of the causal current.

213 Notwithstanding these limitations, it is informative to discuss the implications of our
214 study for the Paleogene paleoceanographic evolution of the eastern Great Australian Bight.
215 Using biostratigraphic proxy data from the Bight and Otway basins, McGowran et al. (1997)
216 suggest the initiation of eastwards protrusion of a so-called ‘proto-Leeuwin Current’ into the
217 Great Australian Bight during the Middle Eocene, with further evidence for its presence in the
218 middle Miocene (Fig. 1A; see also Feary and James, 1995, 1998). This interpretation was,
219 however, challenged by Wyroll et al. (2009), who suggest these fauna may simply record
220 locally elevated sea surface temperatures unrelated to the initiation of a plate-scale
221 thermohaline current. We here suggest Middle Eocene-to-Recent scours and bedforms
222 developed in the Ceduna Sub-basin are associated with Paleogene initiation of an
223 oceanographic current, which we link to the postulated proto-Leeuwin Current. More
224 specifically, we propose these features record late Middle Eocene initiation and subsequent
225 fluctuations in the strength and erosivity of, the current. The major intra-Nullarbor erosion
226 surface (Horizon D), for example, which is best-developed immediately adjacent to the
227 volcanoes, may represent intensification or ‘waxing’ of the proto-Leeuwin Current. Despite a
228 lack of age data, we tentatively suggest this erosional event, and related bedforms, may be the
229 stratigraphic expression of the Miocene Climatic Optimum-related event proposed by Feary
230 and James (1995, 1998), during which time anomalously warm waters encroached eastwards
231 into the Great Australian Bight from western Australian (see also Savin et al., 1975; Gourley
232 and Gallagher, 2004).

233 Our study shows that seismic reflection data can image erosional and depositional
234 features that provide a physical stratigraphic record of ancient ocean currents. We demonstrate
235 that by placing these features into a broad chronostratigraphic framework, we can complement
236 rather sparse micro-faunal evidence, and gain important insights into the timing of onset of
237 major ocean currents. Data limitations notwithstanding, our seismic reflection-based approach

238 does, at the very least, provide a clear hypothesis testable with future scientific drilling (e.g.
239 IODP). Seismic reflection data allow erection of a physical, stratigraphic framework and may
240 be an essential part of the paleoceanographer's toolkit. Future work should focus on detailed
241 mapping of seismic reflection datasets from, for example, the western Bight Basin and Otway
242 Basin; this may reveal similar, age-equivalent current-formed stratigraphic features, thus
243 raising the possibility that the proto-Leeuwin Current extended further eastwards and
244 influenced faunal distribution and potentially climate over a wider area than currently assumed.

245

246 **ACKNOWLEDGEMENTS**

247 Geoscience Australia are thanked for providing seismic and borehole data.

248

249 **REFERENCES**

250

251 Boldreel, L.O.L., Andersen, M.S., and Kuijpers, A., 1998, Neogene seismic facies and deep-
252 water gateways in the Faeroe Bank area, NE Atlantic: *Marine Geology*, v. 152, p. 129-140.

253

254 Callaway, A., Smyth, J., Brown, C.J., Quinn, R., Service, M., and Long, D., 2009, The impact
255 of scour processes on a smothered reef system in the Irish Sea: *Estuarine, Coastal and Shelf
256 Science*, v. 84, p. 409–418.

257

258 Caputi, N., Chubb, C.F., and Pearce, A., 2001, Environmental effects on recruitment of the
259 western rock lobster, *Panulirus Cygnus*: *Marine and Freshwater Research*, v. 52, p. 1167-1175.

260

261 Cann, J.H., and Clarke, J.A.D., 1993, The significance of *Marginopora vertebralis*
262 Foraminifera in surficial sediments at Esperance, Western Australia and in last interglacial
263 sediments in northern Spencer Gulf: *Marine Geology*, v. 111, p. 171–187.

264

265 Cartwright, J.A., and Huuse, M., 2005, 3D seismic technology: the geological 'Hubble'. *Basin
266 Research*, 17, p. 1-20.

267

268 Cresswell, G., and Goldring, T., 1980, Observations of a south-flowing current in the
269 southeastern Indian Ocean: *Deep Sea Research Part 1: Oceanographic Research Papers*, v. 27,
270 p. 449-466.

271

272 Davies, R.J., Cartwright, J.A., Pike, J., and Line, C., 2001, Early Oligocene initiation of North
273 Atlantic deep water formation: *Nature*, v. 410, p. 917-920.
274

275 Due, L., van Aken, H.M., Boldreel, L.O., and Kuijpers, A., 2006, Seismic and oceanographic
276 evidence of present-day bottom-water dynamics in the Lousy Bank-Hatton Bank area, NE
277 Atlantic. *Deep Sea Research Part 1: Oceanographic Research Papers*, v. 53, p. 1729-1741.
278

279 Espurt, N., Callot, J-P., Totterdell, J., Struckmeyer, H., and Vially, R., 2009, Interaction
280 between continental breakup dynamics and large-scale delta system evolution: insights from
281 the Cretaceous Ceduna delta system, Bight Basin, southern Australian margin: *Tectonics*, v.
282 28, TC6002.
283

284 Feary, D.A., and James, N.P., 1995, Cenozoic biogenic mounds and buried Miocene (?) barrier
285 reef on a predominantly cool-water carbonate continental margin, Eucla Basin, western Great
286 Australian Bight: *Geology*, v. 23, p. 427-430.
287

288 Feary, D.A., and James, N.P., 1998, Seismic Stratigraphy and Geological Evolution of the
289 Cenozoic, Cool-Water Eucla Platform, Great Australian Bight: *AAPG Bulletin*, v. 82, p. 792-
290 816.
291

292 Feng, M., Waite, A., and Thompson, P., 2009, Climate variability and ocean production in the
293 Leeuwin Current system off the west coast of Western Australia: *Journal of the Royal Society
294 of Western Australia*, v. 92, p. 67-81.
295

296 Gourley, T.L., and Gallagher, S.J., 2004, Foraminiferal biofacies of the Miocene warm to cool
297 climatic transition in the Port Phillip Basin, southeastern Australia: *Journal of Foraminiferal
298 Research*, v. 34, p. 294-307.
299

300 Henderson, G.M., 2002, New oceanic proxies for paleoclimate, *Earth and Planetary Science
301 Letters*, v. 203, 1-13.
302

303 Hohbein, M., Sexton, P.F., and Cartwright, J.A., 2012, Onset of North Atlantic Deep Water
304 production coincident with inception of the Cenozoic global cooling trend: *Geology*, v. 40, p.
305 255-258.

306

307 Huber, M., Brinkhuis, H., Stickley, C.E., Döös, K., Sluijs, A., Warnaar, J., Schellenberg, S.A.,
308 and Williams, G.L., 2004, Eocene circulation of the Southern Ocean: Was Antarctica kept
309 warm by subtropical waters? *Paleoceanography*, v. 19, PA4026.

310

311 IPCC, 2007, *Climate Change 2007: The physical science basis. Contribution of Working*
312 *Group I to the Fourth Assessment Report of the Intergovernmental Panel on Climate Change*
313 (eds. Solomon, S., Qin, D., Manning, M., Chen, Z., Marquis, M., Averyt, K.B., Tignor, M.,
314 and Miller, H.L). Cambridge University Press, Cambridge.

315

316 Jackson, C.A-L., 2012, Seismic reflection imaging and controls on the preservation of ancient
317 sill-fed magmatic vents: *Journal of the Geological Society*, v. 169, p. 503-506.

318

319 MacLachlan, S.E., Elliott, G.M., and Parsons, L.M., 2008, Investigations of the bottom current
320 sculpted margin of the Hatton Bank, NE Atlantic: *Marine Geology*, v. 253, p. 170-184.

321

322 Magee, C., Hunt-Stewart, E., and Jackson, C.A-L., 2013, Volcano growth mechanisms and the
323 role of sub-volcanic intrusions: Insights from 2D seismic reflection data: *Earth and Planetary*
324 *Science Letters*, 373, p. 41-53.

325

326 McGowran, B., Qianyu, L., Cann, J., Padley, D., McKirdy, D.M., and Shafik, S., 1997,
327 Biogeographic impact of the Leeuwin Current in southern Australia since the late Middle
328 Eocene: *Palaeogeography, Palaeoclimatology, Palaeoecology*, v. 136, p. 19-40.

329

330 O'Reilly, B., Readman, P.W., Shannon, P.M., and Jacob, A.W.B., 2003, A model for the
331 development of a carbonate mound population in the Rockall Trough based on deep-towed
332 sidescan sonar data: *Marine Geology*, v. 198, p. 55-66.

333

334 Rahmstorf, S., 2003, The current climate: *Nature*, v. 421, p. 699.

335

336 Rebesco, M., and Stow, D., 2001, Seismic expression of contourites and related deposits: a
337 preface: *Marine Geophysical Researches*, v. 22, p. 303–308.

338

339 Rollet, N., McGiveron, S., Hashimoto, T., Hackney, R., Petkovic, P., Higgins, K., Grosjean,
340 E., Logan, G.A., 2012, Seafloor features and fluid migration in the Capel and Faust basins,
341 offshore eastern Australia: *Marine and Petroleum Geology*, v. 35, p. 269–291.

342

343 Savin, S.M., Douglas, R.G., and Stehli, F.G., 1975, Tertiary marine paleotemperatures:
344 *Geological Society of American Bulletin*, v. 86, p. 1499–1510.

345

346 Schofield, A., and Totterdell, J., 2008, Distribution, timing and origin of magmatism in the
347 Bight and Eucla basins: Australian Government Report, 2008/24.

348

349 Shafik, S., 1983, Calcareous nannofossil biostratigraphy: an assessment of foraminiferal and
350 sedimentation events in the Eocene of the Otway Basin, southeastern Australia: *Journal of*
351 *Australian Geology and Geophysics*, v. 8, p. 1-17.

352

353 Shafik, S., 1990, The Maastrichtian and early Tertiary record of the Great Australian Bight
354 Basin and its onshore equivalents on the Australian southern margin: a nannofossil study:
355 Bureau of Mineral Resources *Journal of Australian Geology and Geophysics*, v. 11, p. 473-
356 497.

357

358 Stickley, C.E., Brinhuis, H., Schellenberg, S.A., Sluijs, A., Röhl, U., Fuller, M., Grauert, M.,
359 Huber, M., Warnaar, J., and Williams, G.L., 2004, Timing and deepening of the Tasmanian
360 Gateway. *Paleoceanography*, v. 19: PA4027.

361

362 Stow, D.A.V., Faugères, J.C., Howe, J.A., Pudsey, C.J., and Viana, A.R., 2003, Bottom
363 currents, contourites and deep-sea sediment drifts: Current state-of-the-art, in Stow, D.A.V., et
364 al., eds., *Deep-water contourite systems: Modern drifts and ancient series, seismic and*
365 *sedimentary characteristics: The Geological Society of London Memoir*, v. 22, p. 73–84.

366

367 von Blanckenburg, F., 1999, Palaeoceanography: tracing past ocean circulation?: *Science*, v.
368 286, p. 1862-1863.

369

370 Wunsch, C., 2002, What is the thermohaline circulation?: *Nature*, v. 298, p. 1179-1181.

371

372 Wyrwoll, K-H., Greenstein, B.J., Kendrick, G.W., and Chen, G.S., 2009, The
373 palaeoceanography of the Leeuwin Current: implications for a future world. *Journal of the*
374 *Royal Society of Western Australia*, v. 92, p. 37–51.

375

376 **FIGURE CAPTIONS**

377

378 **Fig 1.** (A) Map illustrating the geographical setting of the study area. The area covered by 2D
379 seismic reflection data is outlined by a solid black line. Inset shows the key modern
380 oceanographic currents developed along the western and southern Australian margin.
381 LC=Leeuwin Current; ACC=Antarctic Circumpolar Current; WAC=West Australia Current;
382 FC=Flinders Current. OB=Otway Basin. Modified from Jackson (2012); oceanographic
383 currents from Bilj et al. (2013). (B) Simplified stratigraphic column based on data from
384 boreholes Gnarlyknots-1A and Potoroo-1. Key seismic horizons (A–D) and seismic units
385 (SU1-2) are indicated. The stratigraphic occurrence of intrusion and extrusive components of
386 the Bight Basin Igneous Complex (BBIC) are shown. Modified from Jackson (2012).

387

388 **Fig. 2.** Time-structure map of the Horizon D merged with a time-structure map of Horizon C;
389 this illustrates the distribution of volcano summits (labelled ‘v’ and encircled by a solid white
390 line) that rise above Horizon D, and intra-SU2 moats (labelled ‘m’). sw=sediment wave crests.
391 (A) and (B) are from the southern and northern parts of the study area respectively. See Figure
392 1A for location of map. Light grey lines indicate seismic reflection profiles.

393

394 **Fig. 3.** (A)–(D) Interpreted seismic profiles illustrating the geometry, scale and relationship
395 between extrusive volcanic features of the Bight Basin Igneous Complexes and intra-Nullabor
396 Limestone scours (moats) and bedforms. Locations of the seismic lines are shown in Figure 2.
397 Uninterpreted versions of sections are available in DRI1.

398

399 **Data Repository Item (DR1).** Uninterpreted versions of the seismic profiles presented in Fig.
400 3.

Fig. 1

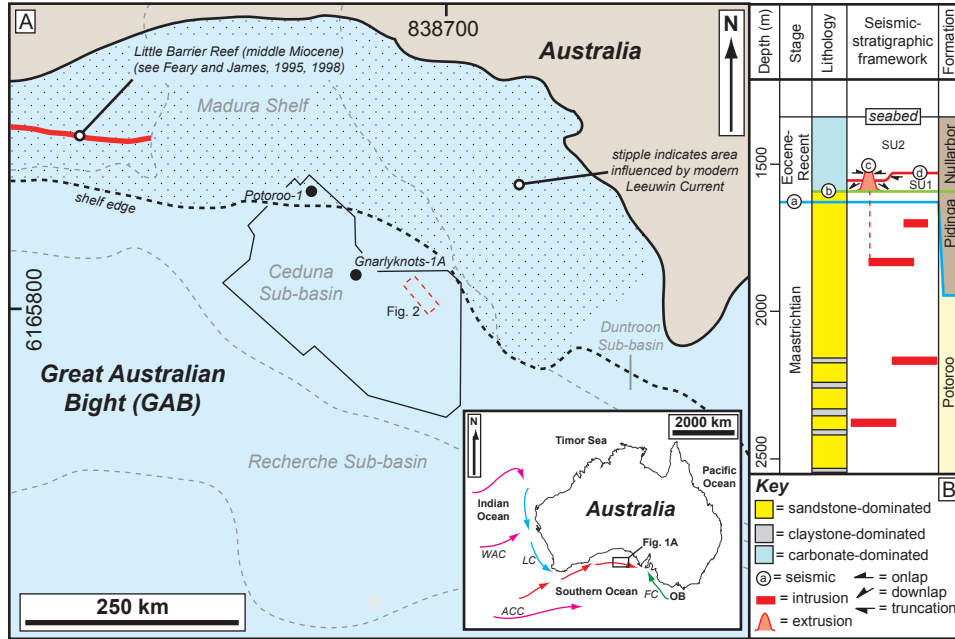


Fig. 2

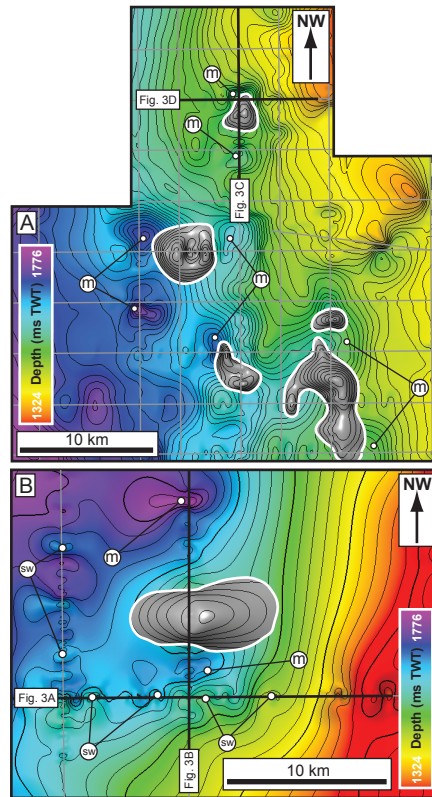
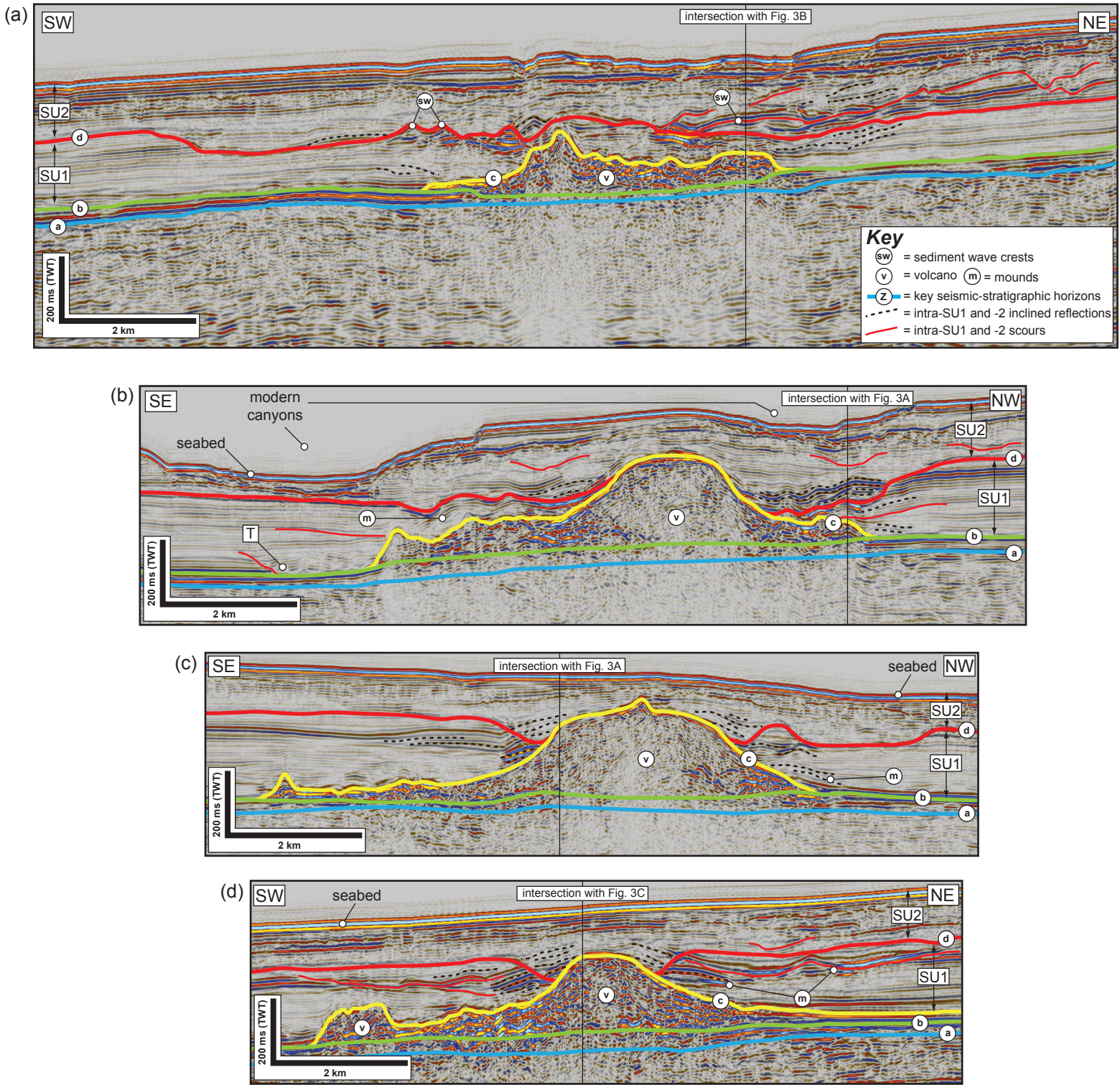


Fig. 3



Data Repository Item 1 (DR1)

